Resonant generation and energetics of wind-forced near-inertial motions in a geostrophic flow

Daniel B. Whitt and Leif N. Thomas

Environmental Earth System Science Department, Stanford University, Stanford, CA

OS31C-1006

1. Introduction

- Mid-latitude storms inject energy into boundary layer inertial oscillations, particularly during the winter season.
- Storm tracks overlie western boundary current extension regions, which contain energetic geostrophic flows and strong fronts.

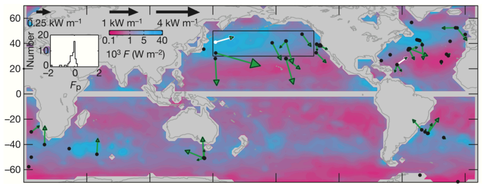

Fig. 1: Colors show annual mean energy input from the wind to mixed-layer near-inertial motions (Alford 2003).

In this paper, we investigate how winds generate inertial oscillations in a laterally sheared geostrophic jet. In that context, we consider the following questions:

1. **How does the geostrophic flow modify the local wind work and resonance conditions for the generation of near-inertial motions?**
2. **Can the mean flow act as an additional source of energy for the forced wave motions?**

2. Inertial motions in a front: a slab mixed layer model

Wave Momentum Time Dependence | Parameterized Radiative Decay | Wind Stress/ Body Force

$$\frac{\partial U_{ML}}{\partial t} - \frac{F^2}{f}V_{ML} = -rU_{ML} + \frac{\tau_x}{\rho H_{ML}} \quad (1a)$$

$$\frac{\partial V_{ML}}{\partial t} + fU_{ML} = -rV_{ML} + \frac{\tau_y}{\rho H_{ML}} \quad (1b)$$

U_{ML}, V_{ML}, τ_x, τ_y function of time only. All other parameters are constant.

Lateral advection of geostrophic momentum is not small in a front
$Ro_g \sim 1$

$$F^2 = f(f - \partial u_g/\partial y) = f^2(1 + Ro_g)$$

- An accurate representation of wave dynamics when wave motions have a low aspect ratio (i.e. low Burger number).
- There is an analytic solution for piecewise constant frequency.
- A change of variables allows the model to be efficiently solved in the frequency domain for an arbitrary set of frequencies.

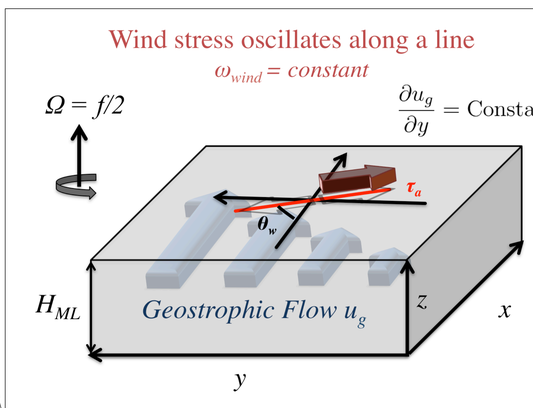

Fig. 2: A schematic illustrating the slab mixed layer problem setup. H_{ML} is the mixed layer depth and τ_a is the amplitude of the wind stress. The wind oscillates back and forth at a fixed angle θ relative to the geostrophic flow and with a fixed frequency ω.

3. Physics of the Slab Mixed Layer Model

Inviscid Initial Value Problem

- Waves exchange energy with the background flow; velocity hodographs are elliptic.
  - However, without damping the wave energy always returns to its initial value.

Dynamics

$$\frac{\partial U_{ML}}{\partial t} - \frac{F^2}{f}V_{ML} = 0, \quad (2a)$$

$$\frac{\partial V_{ML}}{\partial t} + fU_{ML} = 0. \quad (2b)$$

Energetics

$$E_{ML}(t) = \frac{U_{ML}(t)^2 + V_{ML}(t)^2}{2}$$

$$= E_{ML}(0) + \underbrace{\int_0^t -\frac{\partial u_g}{\partial y} V_{ML}(s)U_{ML}(s)\,ds}_{\text{LSP}}$$

Lateral Shear Production

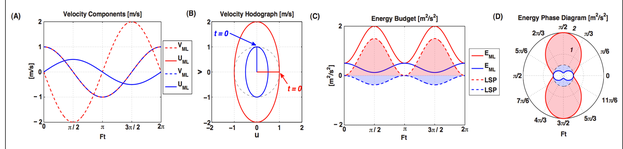

Fig. 3: Velocity (A) and (B) and kinetic energy (C) and (D) for two example inertial oscillations governed by (2a)-(2b). In both examples, Ro_g = -.75 and F/f = 0.5. The perturbation kinetic energy densities, $E_{ML} = 1/2(U_{ML}^2 + V_{ML}^2)$, vary as a function of time/ wave phase as shown in (C) and (D). The oscillations periodically exchange energy with the mean flow via the geostrophic lateral shear production LSP. The blue (red) shaded regions denote negative (positive) LSP.

Forced and Damped Equilibrium

- Governing equations (1a)-(1b) → an under-damped harmonic oscillator.
- Equilibrium dynamics can be interpreted in terms of a response function, which exhibits resonance at the effective Coriolis frequency, $F = f\sqrt{1+Ro_g}$.

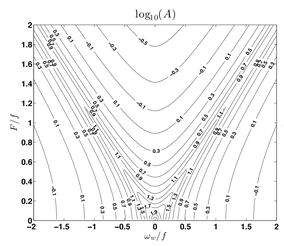

Simple Harmonic Oscillator Equations

$$\frac{\partial^2 V_{ML}}{\partial t^2} + 2r\frac{\partial V_{ML}}{\partial t} + (r^2 + F^2)\,V_{ML} = \frac{1}{\rho_0 H_{ML}}\left(\frac{\partial \tau_y}{\partial t} + r\tau_y - f\tau_x\right)$$

$$\frac{\partial^2 U_{ML}}{\partial t^2} + 2r\frac{\partial U_{ML}}{\partial t} + (r^2 + F^2)\,U_{ML} = \frac{1}{\rho_0 H_{ML}}\left(\frac{\partial \tau_x}{\partial t} + r\tau_x + \frac{F^2}{f}\tau_y\right)$$

Response Function

$$A = \frac{\rho_0 H_{ML} f\,\langle|\mathbf{U}_{ML}^P|\rangle_T}{\langle|\boldsymbol{\tau}|\rangle_T}.$$

< >$_T$ indicates an average over a wave period
$\boldsymbol{U}_{ML}^P$ is the particular solution for the vector velocity

Fig. 4: Response function as a function of forcing frequency and effective Coriolis frequency for winds oscillating perpendicular to the geostrophic flow. H_{ML} = 25 m, r = 5.79x10⁻⁶ s⁻¹, f = 10⁻⁴ s⁻¹,τ_a = 0.06 N/m².

Transient Energetics

- Forcing and damping induce permanent time-integrated energy exchange between waves and geostrophic flow via LSP.
- The sign and magnitude of the time-integrated LSP depends on the angle of the oscillatory wind vector and the Rossby number of the geostrophic flow.

$$E_{ML}(t) - E_{ML}(0) = \underbrace{\int_0^t -\frac{\partial u_g}{\partial y} V_{ML}(s)U_{ML}(s)\,ds}_{\text{LSP}} + \underbrace{\int_0^t -2rE_{ML}(s)\,ds}_{\text{DAMP}} + \underbrace{\int_0^t \frac{\boldsymbol{\tau}(s)\cdot\mathbf{U_{ML}}(s)}{\rho_0 H_{ML}}\,ds}_{\text{WORK}} \quad (3)$$

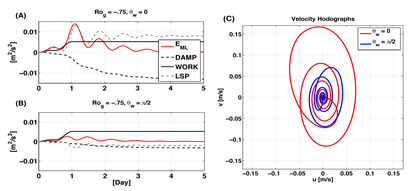

Fig. 5: (A) and (B): Components of (3) integrated over 5 days in two example transient problems. (C) shows the velocity hodographs associated with each case; (A) is red and (B) is blue. In both cases, the forcing WORK is resonant (ω=F) but only active for the first 24 hours, after which the solution follows a homogeneous decay. The LSP is positive and larger than the WORK in (A), but negative and weaker than WORK in (B). In both cases, Ro_g = -.75, H_{ML} = 25 m, r = 5.79x10⁻⁶ s⁻¹, f = 10⁻⁴ s⁻¹,τ_a = 0.06 N/m².

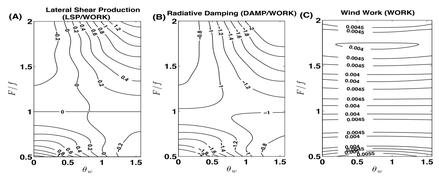

Fig. 6: The terms in (3) integrated over 10 days and plotted after the tenth day as a function of F and the angle of the winds θ_w. The temporal variation of the amplitude of the wind stress is the same as in the example above. The forcing is resonant (ω=F) but only active for the first 24 hours, after which the solutions follow an unforced homogeneous decay. (A) LSP and (B) DAMP are normalized by (C) WORK. All three are order-one contributors to the energy of the perturbation in some parts of parameter space. In all cases, H_{ML} = 25 m, r = 5.79x10⁻⁶ s⁻¹, f = 10⁻⁴ s⁻¹,τ_a = 0.06 N/m².

4. Numerical Simulations

Two questions

- The slab mixed layer model has no explicit lateral spatial variability (it varies only in time). Can the slab model represent inertial oscillation physics accurately when there are realistic horizontal gradients in the slab model parameters?
- The radiative decay parameter *r* is designed to represent both viscous and inviscid physics. Are the results derived with the slab model relevant when there is an ocean below the boundary layer where near-inertial energy may radiate?

Numerical Simulations with Regional Ocean Model

- Simulations confirm that wave energy levels depend strongly on the angle of the oscillatory wind forcing relative to the geostrophic flow.
- Anti-cyclonic flows result in larger energy exchanges for the same relative vorticity magnitude.
- Much of the wave energy decay in the boundary layer is due to inviscid wave propagation.

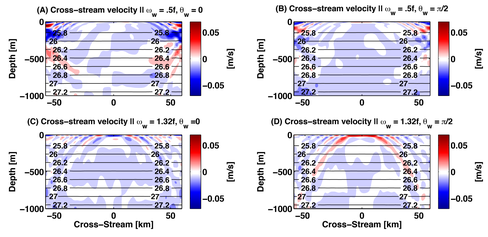

Fig. 7: The cross-stream velocity v, which is all ageostrophic, is plotted in color after 5 days for four numerical simulations with ROMS. The initial condition is a geostrophically balanced barotropic flow: $u_g(y) = U_0\,\sin(2\pi y/L_y)$ where U_0 = 1.5 m/s. The potential density anomaly is contoured in kg/m³. The simulations are forced with a spatially-uniform stress over the first 24 h that oscillates with a fixed frequency and angle as labeled (θ=0 is parallel to x, whereas π/2 is perpendicular) at an amplitude |τ| = 0.06 N/m². Here, Ro_g ranges between +/- 0.8 so he forcing is resonant in the center of the domain in (c) and (d) and on the edges in (a) and (b). All variables are uniform in the x direction.

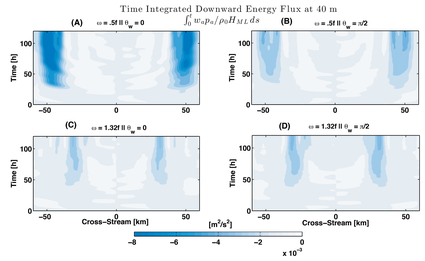

Fig. 8:The time-integrated downward wave energy flux evaluated just below the boundary layer and plotted as a function of time and cross-stream position in the four ROMS simulations above. In this case, p_a is the pressure perturbation (from the time mean), w_a is the vertical velocity, and H_{ML}= 40 m is the approximate depth of the boundary layer, an output of the K-profile-parameterization mixing scheme.

Comparison between Slab Model and Simulations

- The slab model both qualitatively and quantitatively reproduces the results in the numerical simulations even though the wave decay is largely inviscid.
- In strongly anti-cyclonic jets, geostrophic shear production can dominate the wind work as a wave energy source when the winds are oriented parallel to the jet.

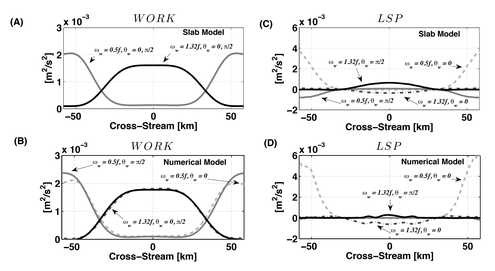

Fig. 9: The 5-day-integrated WORK, (A) and (B), and LSP, (C) and (D), in the 4 cases above. (A) and (C) are computed with the slab model, whereas (B) and (D) are computed with the numerical mode. In the slab model, H_{ML} = 40 m, r = 5.79x10⁻⁶ , and f = 10⁻⁴ s⁻¹.

The equivalent mixed layer velocity in the numerical model is computed as

$$\mathbf{U}_{\mathrm{ML}}(t) = 1/H_{\mathrm{ML}} \int_{-H_{\mathrm{ML}}}^{0} \mathbf{u}_g(t,z)\,dz$$

where H_{ML} = 40 m in this case.

5. Broader Implications

- An ensemble of inviscid inertial oscillations in a geostrophic flow with finite Rossby number and a uniform distribution of initial phases but constant initial amplitude, will have a time and ensemble-averaged energy greater than the initial energy.

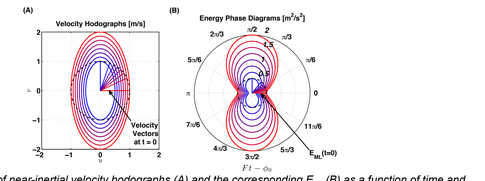

Fig. 10: An ensemble of near-inertial velocity hodographs (A) and the corresponding E_{ML} (B) as a function of time and initial phase angle ϕ_0. As in Fig. 2, the background flow is characterized by Ro_g = −0.75 and the initial speed of each oscillation is the same 1 m/s (dashed black circle) but the initial perturbation velocity vector has a different angle in each case. The energy averaged over a wave period varies substantially with ϕ_0, and when additionally averaged over all initial phase angles ϕ_0 it exceeds the average initial energy .5 m²/s² (dashed black circle in (B)).

- Similarly, an ensemble of near-inertial motions forced by an isotropic distribution of wind angles will always result in a net extraction of energy from a geostrophic jet at any finite Rossby number.

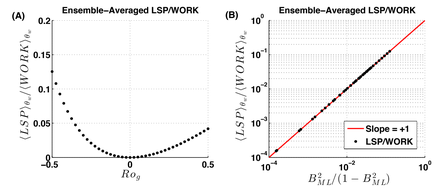

Fig. 11: The θ-ensemble-average lateral shear production $\langle LSP\rangle_{\theta_w}$ as a function of (A) Ro_g and (B) $B_{ML}^2/(1-B_{ML}^2) = Ro_g^2/4(1+Ro_g)$. Both panels show $\langle LSP\rangle_{\theta_w}$ normalized by the ensemble-average wind work $\langle WORK\rangle_{\theta_w}$ where the average is taken over a large ensemble of ten-day transient spin-up/spin-down integrations, as in Fig 9 with a uniform distribution of wind orientation angle θ ∈ [−π, π) and resonant forcing for the first 24 hours. H_{ML} = 25 m, r = 5.79x10⁻⁶ s⁻¹, f = 10⁻⁴ s⁻¹,τ_a = 0.06 N/m².

$$\langle LSP\rangle_{\theta_w} \sim \langle WORK\rangle_{\theta_w} \frac{B_{ML}^2}{1-B_{ML}^2} = \langle WORK\rangle_{\theta_w} \frac{Ro_g^2}{4(1+Ro_g)}.$$

- The net energy exchange scales as the wind work times Ro_g^2, so estimates for the geostrophic contribution to global near-inertial energy based on this mechanism range from about 1% of the wind-work (based on the vorticity distribution of Rudnick (2001) in the Pacific subtropical gyre) to 30% of the wind work (based on the vorticity distribution of Shcherbina et al. (2013) in the Sargasso Sea just southeast of the Gulf Stream during winter).
- More research is needed to study these dynamics in non-rectilinear geostrophic flows, such as eddies and meanders, and to consider the effect of the forced/dissipating waves on the mean flow.

6. Key Results

- Geostrophic vertical vorticity changes the resonant frequency for near-inertial motion (Fig. 4). In a rectilinear jet, this effective Coriolis frequency is given by

$$F = f\sqrt{1+Ro_g}$$

- Near-inertial motions exchange energy with the geostrophic flow via lateral shear production at finite Rossby number.
- In geostrophic jets with O(1) Rossby number, the time averaged lateral shear production can be larger than the wind work (e.g. Figs. 5, 6 and 9).
- The sign and magnitude of the lateral shear production depends strongly on the angle of the winds relative to the geostrophic flow. However, an ensemble of isotropically distributed wind forcing angles always results in an extraction of energy from the geostrophic flow to the waves at finite Rossby number (Fig. 11).
- Numerical simulations confirm analysis derived from an analytic slab mixed layer model and show that the time-integrated energy exchange is robust and occurs even when much of the "damping" in the slab model is due to inviscid wave radiation from the boundary layer to the ocean interior (Figs. 7-9).

6. References

Alford, M. (2003), Redistribution of energy available for ocean mixing by long range propagation of internal waves, *Nature*, 423, 159-162.

Rudnick, D. (2001), On the skewness of vorticity in the upper ocean, Geophys. Res. Lett., 28, 10, 2045-2048.

Shcherbina, A. Y., E. A. D'Asaro, C. M. Lee, J. M. Klymak, M. J. Molemaker, and J. C. McWilliams (2013), Statistics of vertical vorticity, divergence, and strain in a developed submesoscale turbulence field, Geophys. Res. Lett., 40, 4706–4711, doi:10.1002/grl.50919

Whitt, D. B., and L. N. Thomas (2014), Resonant generation and energetics of wind-forced near-inertial motions in a geostrophic flow. *J. Phys. Oceanogr.* doi:10.1175/JPO-D-14-0168.1, *in press.*